Bioconjugate Chemistry

Article

pubs.acs.org/bc

Optimized Design and Synthesis of a Cell-Permeable Biarsenical Cyanine Probe for Imaging Tagged Cytosolic Bacterial Proteins

Na Fu, Yijia Xiong, and Thomas C. Squier*

Biological Sciences Division, Fundamental Sciences Directorate, Pacific Northwest National Laboratory, Richland, Washington 99352, United States

Supporting Information

ABSTRACT: To optimize cellular delivery and specific labeling of tagged cytosolic proteins by biarsenical fluorescent probes built around a cyanine dye (Cy3) scaffold, we have systematically varied the polarity of the N-alkyl chain (i.e., 4−5 methylene groups appended by a sulfonate or methoxy ester moiety) and arsenic capping reagent (ethanedithiol versus benzenedithiol). Optimal live-cell labeling and visualization of tagged cytosolic proteins is reported using an ethanedithiol capping reagent with the uncharged methoxy ester functionalized N-alkyl chains. These measurements demonstrate the general utility of this new class of photostable and highly fluorescent biarsenical probes based on the cyanine dye scaffold for in vivo labeling of tagged cellular proteins for live cell imaging measurements of protein dynamics.

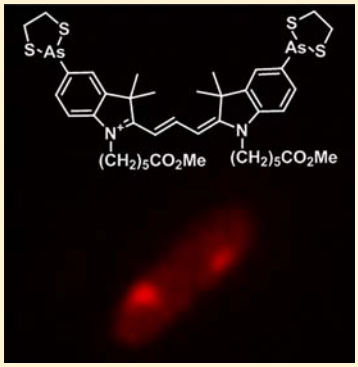

INTRODUCTION

Cell-permeable chemical probes permit the routine targeted labeling of tagged intracellular proteins in living cells. There are two classes of commercially available labeling reagents useful for a wide variety of cell types involving: (i) metabolically activated fluorescent substrates that are recognized by genetically encoded enzymes appended to proteins of interest, e.g., SNAP[1−5] and Halo,[6] or (ii) biarsenical reagents (e.g., FlAsH) that selectively bind to short peptide sequences engineered into the proteins of interest that contain pairs of vicinal cysteines.[7−11] In the case of the SNAP and Halo technologies, the appended enzymes (O_6-alkylguanine DNA alkyltransferase and haloalkane dehalogenase) have a primary advantage over the use of genetically encoded fluorescent proteins in that they permit pulse-chase measurements of protein synthesis and localization, as substrates can be modified with different fluorophores. However, the large sizes of these appended proteins can also interfere with protein complex formation and cellular targeting.[7,12] In comparison, biarsenical probes bind to short (9−15 amino acid) engineered tetracysteine tags that allow correct protein localization and the formation of biologically relevant protein complexes.[13]

Commercially available biarsenical fluorescent probes with a conserved interarsenic separation of about 5 Å permit targeted labeling of tagged cellular proteins for live-cell imaging, but have been limited by the availability of a single class of reagents, which bind to one tetracysteine tagging motif (i.e., CCPGCC).[7,10,11,14] Sequence variations proximal to the viscinal cysteines have permitted multicolor measurements using available biarsenical dyes FlAsH and ReAsH in measurements of protein−protein interactions;[15,16] however, these applications involve relatively modest differences in binding affinity that prevent their robust utility. To enhance the ability to discriminate tagging sequences, we have previously developed a class of biarsenical probes (AsCy3) built around a cyanine dye scaffold with an interarsenic separation of 14.5 Å that bind to orthogonal tetracysteine tags (CCKAEAACC). Thus, multicolor measurements can be achieved by simultaneously using orthogonal biarsenical probes to selectively monitor the structural dynamics of individual proteins in a complex,[9] but are currently limited by the inability to use AsCy3 for live cell measurements due to either poor intracellular delivery or nonspecific biomolecular binding.

To enhance the utility of AsCy3 for cellular imaging applications, we have synthesized a family of probes that systematically vary the polarity of the terminal groups of the N-alkyl chains and the arsenic capping reagent (Scheme 1). **AsCy3_E** with both an ethanedithiol cap and uncharged methoxy ester functionalized N-alkyl chains demonstrates optimal utility for targeting tagged proteins (Scheme 2), indicating that specific labeling is achieved by reducing the polarity of the biarsenical cyanine probe to optimize delivery, while retaining sufficient polarity to maintain specific targeting to introduced tagging sequences. Specificity of labeling is demonstrated for two cytosolic proteins, namely, the α-subunit of RNA polymerase (RpoA*) that forms a limited number of foci in the cell under optimal growth conditions that are indicative of the formation of supramolecular complexes,[17,18] and a cytosolic peptidyl-prolyl cis−trans isomerase protein SlyD that is visualized as diffuse staining, consistent with its

Received: November 21, 2012
Revised: January 14, 2013
Published: January 21, 2013

dx.doi.org/10.1021/bc300619m | *Bioconjugate Chem.* 2013, 24, 251−259

Scheme 1. Synthesis of Biarsenical Probes[a]

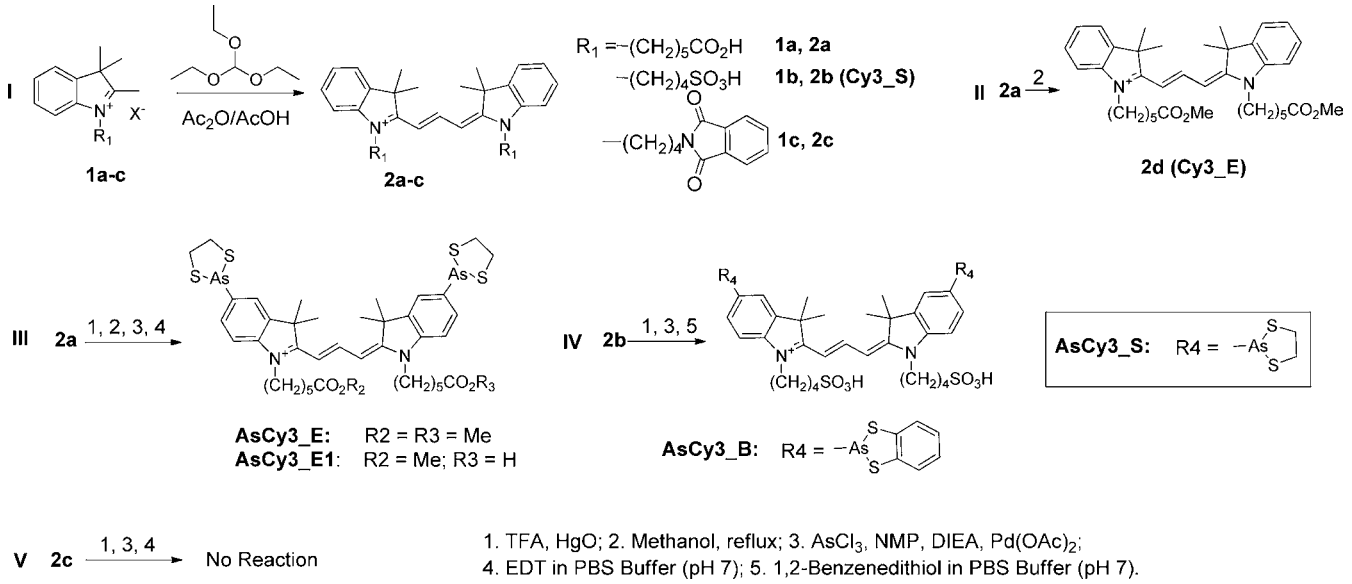

[a]A rectangle is drawn around the structure of **AsCy3_S**, whose synthesis was previously reported.[9]

Scheme 2. Depiction of Bioconjugation Reaction between Biarsenical Cyanine Probe AsCy3_E and Nine Amino Acid Tetracysteine Fusion Tag (i.e., CCKAEAACC)

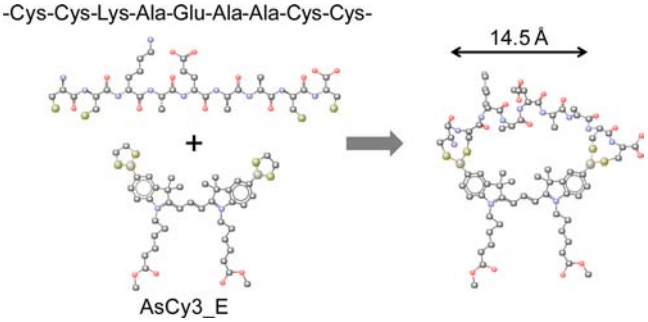

general role in facilitating protein folding and correct metal insertion during protein maturation.

EXPERIMENTAL PROCEDURES

Synthesis of Cyanine Dyes. Cyanine dyes **2a**, **2b**, and **2c** were synthesized essentially as previously described,[19] which involved heating the corresponding quaternary salts (**1a–c**) with triethyl orthoformate in buffered acetic anhydride/acetic acid (1.5 mL acetic acid, 1.1 mL acetic anhydride, and 0.065 g sodium acetate) at 120 °C. The resulting mixtures were dissolved in CH_2Cl_2, washed by water, dried under reduced pressure, and the residue was purified by chromatography on silica gel using methanol in methylene dichloride as eluent. Product identity was confirmed using NMR, which we report for cyanine **2a** and **2c** (see below). Properties of **2b** were reported previously.[9]

*Cyanine **2a**.* (70% yield). ^{1}H NMR ($CDCl_3$): δ 1.56 (m, 4H), 1.75 (m, 4H), 1.77 (s, 12H), 1.86 (m, 4H), 2.35 (t, J = 7.5 Hz, 4H), 4.07 (t, J = 7.5 Hz, 4H), 6.33 (d, J = 14 Hz, 2H), 7.20 (d, J = 9 Hz, 2H), 7.32 (d, J = 7 Hz, 2H), 7.41–7.47 (m, 4H), 8.45 (t, J = 13 Hz, 1H). MS (ESI): m/z: 557.3 $[M]^+$.

*Cyanine **2c**.* (95% yield). ^{1}H NMR ($CDCl_3$): δ 1.72 (s, 12H), 1.95 (m, 4H), 2.05 (m, 4H), 3.67 (t, J = 6 Hz, 4H), 4.34 (t, J = 6 Hz, 4H), 6.73 (d, J = 7.5 Hz, 2H), 7.19 (d, J = 7.5 Hz, 2H), 7.34–7.39 (m, 6H), 7.71 (m, 4H), 7.81 (m, 4H), 8.44 (t, J = 13 Hz, 1H). MS (ESI): m/z: 731.4 $[M]^+$.

*Cyanine **2d**.* (70% yield). 10 mL methanol was added to the crude compound **2a** and refluxed for 1 h. Then the solvent was removed and the residue was dried under high vacuum and purified by chromatography on silica gel using methanol in methylene dichloride as eluent (gradient of 0–5%) ^{1}H NMR ($CDCl_3$): δ 1.63 (m, 4H), 1.70 (s, 12H), 1.73 (m, 4H), 1.88 (m, 4H), 2.36 (t, J = 7.5 Hz, 4H), 3.60 (s, 6H), 4.27 (t, J = 7.5 Hz, 4H), 7.10 (d, J = 7.5 Hz, 2H), 7.22 (t, J = 7.5 Hz, 2H), 7.36–7.40 (m, 4H), 7.51 (d, J = 12.5 Hz, 2H), 8.41 (t, J = 13 Hz, 1H) MS (ESI): m/z: 585.4 $[M]^+$.

Synthesis of AsCy3_E and AsCy3_E1. Compound **2a** (167 mg, 0.3 mmol) was added into trifluoroacetic acid containing mercuric oxide (1.3 g, 6 mmol) at room temperature. After 48 h stirring, 4 mL methanol was added to the mixture and refluxed for 0.5 h. Then, the solvent was removed and the residue was dried under high vacuum. A purple solid was suspended in dry *N*-methylpyrrolidone (3 mL) with arsenic trichloride (500 μL, 6 mmol), diisopropylethyl amine (280 μL, 1.6 mmol), and catalytic palladium acetate (1 mg). The reaction was stirred at room temperature for 8 h. After reaction, 5 mL phosphate buffer pH 7 and 1,2-ethanedithiol (535 μL, 6.4 mmol) were added into the reaction mixture. The solution was extracted with CH_2Cl_2 (3 × 30 mL), dried over Na_2SO_4, evaporated, and purified by chromatography on silica gel using methanol in methylene dichloride as eluent (gradient of 0–10%).

***AsCy3_E**.* (20% yield). ^{1}H NMR ($CDCl_3$): δ 1.63–1.71 (m, 20H), 1.85 (m, 4H), 2.35 (t, J = 6.0 Hz, 4H), 3.19 (m, 4H), 3.40 (m, 4H), 3.63 (s, 6H), 4.21 (m, 4H), 7.08–7.23 (m, 6H), 7.60 (m, 2H), 8.38 (t, J = 13.5 Hz, 1H). MS (ESI): m/z: 917.2 $[M]^+$.

***AsCy3_E1**.* (18% yield). ^{1}H NMR ($CDCl_3$): δ 1.51 (m, 2H), 1.59 (m, 2H), 1.67 (m, 2H), 1.72 (s, 12H), 1.83 (m, 6H), 2.32 (t, J = 7.5 Hz, 2H), 2.51 (t, J = 7.5 Hz, 2H), 3.18 (m, 4H), 3.41 (m, 4H), 3.64 (s, 3H), 4.07 (m, 2H), 4.16 (m, 2H), 6.70 (d, J = 12.5 Hz, 1H), 6.86 (d, J = 12.5 Hz, 1H), 7.06–7.11 (m, 2H),

dx.doi.org/10.1021/bc300619m | *Bioconjugate Chem.* 2013, 24, 251–259

7.61−7.71 (m, 4H), 8.34 (t, J = 12.5 Hz, 1H). MS (ESI): m/z: 903.1 $[M]^+$.

Synthesis of AsCy3_B. Compound **2b** (180 mg, 0.3 mmol) was added into trifluoroacetic acid containing mercuric oxide (1.3 g, 6 mmol) at room temperature. Then, the solvent was removed and the residue was dried under high vacuum. The resulting purple solid was suspended in dry *N*-methylpyrrolidone (3 mL) with arsenic trichloride (500 μL, 6 mmol), diisopropylethyl amine (280 μL, 1.6 mmol), and catalytic palladium acetate (1 mg). The reaction was stirred at room temperature for 8 h. After reaction, 5 mL of phosphate buffer (pH 7) and 1,2-benzenedithiol (735 μL, 6.4 mmol) were added into the reaction mixture. The solution was extracted with CH_2Cl_2 (3 × 30 mL), dried over Na_2SO_4, evaporated, and purified by chromatography on silica gel using methanol in methylene dichloride as the eluent (gradient of 0−5%) with an 28% yield.

AsCy3_B. ^{1}H NMR ($CDCl_3$): δ 1.57 (s, 12H), 1.79 (m, 4H), 1.92 (m, 4H), 2.91 (t, J = 7.5 Hz, 4H), 4.10 (m, 4H), 6.50 (d, J = 12.5 Hz, 2H), 6.98 (m, 4H), 7.14 (d, J = 7.5 Hz, 2H), 7.39 (m, 4H), 7.56 (s, 2H), 7.60 (d, J = 7.5 Hz, 2H), 8.28 (t, J = 13.5 Hz, 1H). MS (ESI): m/z: 1029.0 $[M]^+$.

Cloning and Expression of the α-Subunit of RNA Polymerase in *E. coli*. A C-terminal 52-amino-acid sequence was appended onto the α-subunit of RNA polymerase (RpoA) cloned into the pBAD202/D-TOPO vector (Invitrogen) containing in the following order a tetracysteine tag CCKAEAACC adjacent to a V5 epitope (KGGRADPA-FLYKVVINSKLEGKPIPNPLLGL) and a His_6 sequence at the C-terminus, essentially as previously described.[17] The tagged α-subunit of the RNA polymerase (RpoA*) was expressed in *E. coli* using the pBAD/D-TOPO expression system contains the promoter of the araBAD (arabinose) operon, which can be upregulated by arabinose and down-regulated by glucose to permit optimal expression. Plasmids were maintained by addition of 50 μg/mL kanamycin. Typically, a stock culture of *E. coli* expressing RpoA-AsCy3TAG was streaked on selective agar plates containing kanamycin and incubated for 16 h at 37 °C. One colony was picked using a sterile plastic loop and upon inoculation into 5 mL of LB with kanamycin (50 μg/mL) was placed in a 37 °C shaker incubator for eight hours. An aliquot (5 μL) was then transferred to 5 mL fresh LB with antibiotics and grown at 37 °C in a shaker until OD_{600} = 0.6. For induction of tagged RpoA, 5 μL of 1 M arabinose (1 mM final concentration) was added and the tube was incubated for another three hours at 37 °C. As a control, a cell culture without induction was prepared in parallel.

Cell Lysis. *E. coli* cell suspensions were subjected to six freeze−thaw cycles involving freezing in liquid nitrogen followed by thawing at a 37 °C water bath prior to centrifugation at 17 200*g* for 25 min to remove cell debris. The lysis buffer contained 25 mM HEPES (pH 7.6). Protein concentrations of lysate were measured using a BCA assay kit (Pierce) prior to freezing samples at −80 °C for storage.

Affinity Purification of RpoA*. Lysates were passed over a Histrap Ni-sepharose 6 FF column (GE healthcare, 1 mL) pre-equilibrated with Buffer A [25 mM HEPES (pH 7.5), 0.3 M NaCl, and 10% glycerol (v/v)] + 25 mM imidazole. The column was washed once with 10 mL of buffer A + 25 mM imidazole and a second time with 10 mL of buffer A + 75 mM imidazole. Affinity purified RpoA* was eluted upon addition of buffer A + 250 mM imidazole.

Labeling of Purified RpoA* with Biarsenical Probes. Isolated RpoA* in 25 mM HEPES (pH 7.5), 0.3 M NaCl, 0.25 M imidazole, 5 mM TCEP, and 10% glycerol (v/v) was incubated in the presence of indicated concentrations of **AsCy3_B**, **AsCy3_S**, or **AsCy3_E** for one hour at room temperature.

Cell Labeling. Freshly cultured bacterial cells (2 mL) were incubated for 30 min at room temperature with **AsCy3_E** (0.5 μM unless otherwise indicated) in the presence of Disperse Blue (20 μM). After labeling, excess probe was removed from bacterial cells through eight sequential washing steps involving centrifugation of cells (2 mL) for one minute at 14 000*g* prior to resuspension. Washing steps involved 2× with 25 mM HEPES (pH 7.6), 2× with 5 mM β-mercaptoethanol in 25 mM HEPES (pH 7.6), 2× with 2.5% BSA (w/v) in 25 mM HEPES (pH 7.6), and 2× with 25 mM HEPES (pH 7.6). Finally, cells were brought up in 200 μL of 25 mM HEPES buffer (pH 7.6) for further analysis.

Fluorescence Imaging of Cyanine Probes in Living Cells. Live-cell imaging of labeled proteins involved sealing a coverslip following placement of *E. coli* (1 μL) onto a microscope slide, taking care to exclude air bubbles. Bright-field and fluorescent images were sequentially collected soon after fluorescent labeling of *E. coli*, where the focus was first set using the bright-field image prior to obtaining the fluorescence image. Differences in the sharpness of the images arise, in part, due to the fact that we are imaging living cells, where cells move during the collection of the fluorescent image (which takes about 1 s). In comparison, bright-field images were collected on the millisecond time-scale, during which there is minimal cell movement. Images were taken using a Nikon eclipse Ti−U inverted microscope equipped with a 60× Nikon Plan Apo oil immersion objective (NA = 1.4) and a Coolsnap HQ charge-coupled device camera (Photometrics). The excitation source was a white LED module from Thorlabs (LEDC19) and fluorescence images were acquired using a standard set of band-pass filters for Cy3 (Nikon).

RESULTS

Design Strategy. The influence of different functional groups that modify the hydrophobicity of the biarsenical cyanine probe was systematically explored to enable enhanced cellular delivery. Alkylation of the heterocyclic precursor permits introduction of different functional groups to the cyanine dye scaffold prior to the mercuration and trans-metalation reaction with As(III). Carboxylic, sulfonic acid, and phthalimide were chosen as desired functionalities because of their altered hydrophobicity and chemical inertness toward the reagents and reaction conditions needed for condensation reactions. Carboxylic functionalities were methylated to modify probe hydrophobicity, where endogenous esterases are expected to cleave the methoxy esters to enhance solubility following cellular delivery, thus minimizing hydrophobic interactions with nontarget proteins.[8,20,21] Additional structural diversity involved altering the ligand cap stabilizing the arsenic motif from the commonly used ethanedithiol (EDT) to consider the more hydrophobic benzenedithiol.

Synthesis. The core biarsenical scaffold, Cy3, was prepared in two steps using standard cyanine dye synthesis protocols involving indolium salts as a precursor.[22] Generally, the precursor was obtained by reacting 2,3,3-trimethylindolenine with excess alkyl halides in anhydrous 1,2 dichlorobenzene at 120 °C, followed by chromatographic purification with decent

yield; 60% and 70% for compound **1a** and **1b**, respectively (Scheme 1). Synthesis of precursor **1c** involved heating equistoichiometric amounts of *N*-(4-bromobutyl) phthalimide and 2,3,3-trimethylindolenine in a pressure tube without solvent at 140 °C with stirring;[23] a quantitative yield was obtained without purification. Formation of cyanine dyes was accomplished by a condensation reaction of the corresponding quaternary indolium salts and triethyl orthoformate in buffered acetic anhydride/acetic acid at 120 °C, where consistently good yields were obtained: 70%, 90%, and 95% for compound **2a**, **2b**, and **2c**, respectively, after chromatographic purification. Facile formation of the methoxyester derivative **2d** (**Cy3_E**) occurs in methanol.

In all cases, the cyanine dyes were mercurated in trifluoric acid with two equivalents of mercury oxide, followed by the transmetalation of arsenic and subsequent stabilization by appropriate capping ligands ethandithiol (EDT) or 1,2-benzenedithiol to afford the final biarsenical probes[9] (i.e., **AsCy3_E**, **AsCy3_S**, and **AsCy3_B**). Significantly different reactivities are observed for the mercuration and transmetalation reaction depending on the functional groups introduced onto the cyanine dye scaffolds. Cyanine dyes **2a** and **2b** give good overall yields; in comparison, **2c** shows no reactivity even over a prolonged reaction time. Likewise, no reaction is observed upon inclusion of a methyl group as a side chain (data not shown), suggesting the importance of an ionizable group for effective reactivity. This observation is consistent with prior reaction mechanisms that suggest an electrophilic reaction between the mercurating agent and aromatic hydrocarbons that arises due to the stabilization of an arenium ion intermediate.[24] Such insights suggest that ionizable functional groups incorporated onto the cyanine scaffold are critical to stabilize the intermediate indolmercurenium ions to enhance reactivity to favor the subsequent transmetalation reaction.

To facilitate cellular delivery, the polarity of the biarsenical probe with carboxylate moieties was reduced through synthesis of methoxyester derivatives. As ionic N-alkyl chains were required for the mercuration reaction, esterification was performed following mercuration of **2a** by refluxing the reactant in methanol for 30 min prior to the transmetalation reaction. The final separated products include diester and monoester products **AsCy3_E** and **AsCy3_E1** in yields of 20% and 18%, respectively. Increasing the duration of refluxation enhanced the yield of the **AsCy3_E** diester over the **AsCy3_E1** monoester; the monoester represents a desired product with increased water solubility that has the capability for additional coupling reactions.[25]

Spectroscopic Characterization. In ethanol, there is a 14−17 nm red-shift in the absorbance and fluorescence emission maxima of the biarsenical probes accompanying modest increases in the quantum yield in comparison with the precursor cyanine dye (Table 1). The absorbance and fluorescence spectra of the biarsenical probes are essentially insensitive to the introduced scaffold modifications, resulting in minimal spectral shifts irrespective of the rigidity of the arsenic capping moiety or the functionality of the alkyl chain. Introduction of the more rigid aromatic ligand cap decreases the quantum yield of **AsCy3_B** in ethanol by about 25% in comparison to either **AsCy3_S** or **AsCy3_E**, consistent with prior indications that more rigid capping rings modify ring strain to reduce the fluorescence of other biarsenical probes (i.e., FlAsH).[15] The spectroscopic properties of the biarsenical probes **AsCy3_S** and **AsCy3_E** are largely preserved in aqueous solution, where small spectral shifts and 40−50% reductions in the quantum yields are consistent with observed changes in the photophysical properties of the parent Cy3 dye (Table 1; Figure 1). However, **AsCy3_B** exhibits a red-shift J-aggregation peak in aqueous solution due to a $\pi-\pi$ stacking interaction between the benzene ring and cyanine that is apparent from observed changes in the absorption spectrum.[26]

Table 1. Photophysical Properties of Synthesized Probes[a]

solvent	compound[b]	λ_{abs} [nm]	λ_{em} [nm]	Φ_f
ethanol	**2b**	548	562	0.08
	AsCy3_S	566	580	0.13
	AsCy3_E	562	578	0.12
	AsCy3_B	568	582	0.09
PBS[c]	**2b**	544	558	0.05
	AsCy3_S	560	572	0.07
	AsCy3_E	556	570	0.06
	AsCy3_B	555, 584[d]	570	-
PBS	**AsCy3_S·RpoA***	567	575	0.14
	AsCy3_E·RpoA*	565	579	0.21
	AsCy3_B·RpoA*	567	578	0.12

[a]Fluorescence quantum yields were determined using Rhodamine 6G as the standard (Φ_f = 0.95 in ethanol). [b]Spectral properties of biarsenical probes were assessed free in solution or following binding to RpoA*. [c]PBS buffer (pH 7.4) includes 5% DMSO. [d]J-aggregation peak observed at 584 nm. λ_{ex} = 500 nm for fluorescence measurements.

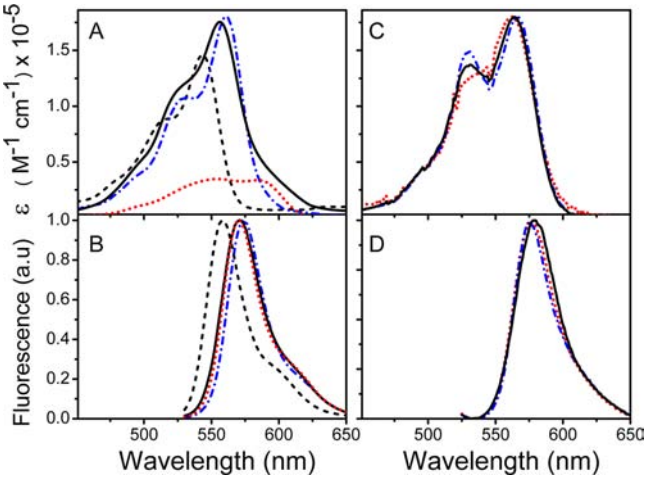

Figure 1. Spectral Sensitivity of Biarsenical Cyanine Probes to Introduced Modifications. Absorbance (top) and normalized fluorescence emission (bottom) spectra for biarsenical cyanine probes in solution (panels A, B) or following binding to RpoA* (panels C, D) for **Cy3_S** (2b) (dashed black line), **AsCy3_S** (dash-dotted blue line), **AsCy3_E** (solid black line), and **AsCy3_B** (dotted red line) in aqueous buffer [5% (v/v) DMSO and 25 mM Na_2HPO_4 (pH 7.4)]. All concentrations of biarsenical probes were 1 μM (absorbance spectra) or 20 nM (fluorescence emission spectra). Absorbance spectra in panel C are normalized relative to that of unbound **AsCy3_S** in panel A. Excitation wavelength was 510 nm. Relative differences in quantum yields are summarized in Table 1.

To assess spectral changes upon protein binding, we have engineered a tetracysteine binding sequence (CCKKAEAACC) at the C-terminus of the α-subunit of RNA polymerase (RpoA*), at a site previously shown to be compatible with high-affinity binding using other biarsenical probes.[17] Upon

dx.doi.org/10.1021/bc300619m | *Bioconjugate Chem.* 2013, 24, 251−259

displacement of the arsenic capping moieties (i.e., ethanedithiol or 1,2-benzenedithiol) upon binding to RpoA*, there is a red shift in both absorbance and fluorescence emission spectra (Figure 1). Resulting spectra of all three AsCy3 probes are very similar to each other following binding to RpoA*. Upon correction for differences in labeling stoichiometries for AsCy3 bound to RpoA*, which varies between 0.12 (**AsCy3_B**), 0.48 (**AsCy3_S**), and 0.52 (**AsCy3_E**) (see Figure S3), there is a 3.5-fold increase in the fluorescence quantum yield of **AsCy3_E** upon binding RpoA*; in comparison, the quantum yields of **AsCy3_S** and **AsCy3_B** increase by about 2-fold upon target protein binding (Table 1). Increases in the quantum yields of all three AsCy3 probes upon binding RpoA* are consistent with a stabilization of a highly fluorescent Cy3 conformer, which is further enhanced upon a reduction in the polarity of the N-alkyl methoxy ester chain in **AsCy3_E** in comparison to the sulfonate moieties in **AsCy3_S** or **AsCy3_B**.[27]

Cell Permeability and Protein Targeting. To assess the utility of the synthesized biarsenical probes for intracellular delivery and visualization of protein complexes in living cells, RpoA* was expressed in the cytosol of *E. coli* at near native abundance (1%), permitting a determination of the labeling specificity and utility of these biarsenical cyanine probes. Under these expression conditions, prior measurements have demonstrated the formation of supramolecular complexes involving RNA polymerase that form near the membrane under rapid growth conditions, acting to overcome diffusional constraints to promote metabolic efficiencies involving the efficient production of stable RNA (rRNA and tRNA) necessary for ribosome assembly and protein synthesis, which limit overall growth rates in rich media.[17,18,28,29] In comparison, under conditions that limit growth, RNA polymerase appears as a more diffuse cellular distribution that is indicative of shifts in the distribution of RNA polymerase to enhance the transcription of mRNA under conditions where rates of protein synthesis do not limit growth.[17,18,28,29] This latter diffuse distribution is similar to that expected for other cytosolic proteins such as SlyD that contains a naturally occurring high-affinity tetracysteine binding sequence (GCCGGHGHDHGHEHGGEG CCGG),[30] permitting labeling of a protein with a broad cytosolic distribution.

In the absence of RpoA* induction (i.e., no arabinose in the media), SlyD is specifically labeled upon live-cell incubation of *E. coli* with **AsCy3_E**, as evidenced by a 24 kDa fluorescent band apparent following cell lysis and protein separation by SDS-PAGE (Figure 2C). Upon induction of RpoA* and live-cell incubation of *E. coli* with **AsCy3_E**, a prominent fluorescent band with an apparent molecular mass of 42 kDa is labeled in addition to SlyD (Figure 2C).[17,30] Equivalent specificity of labeling is apparent using **AsCy3_S** and **AsCy3_B** following optimization of labeling (Figure 2; Figure S1 in Supporting Information). In contrast, no proteins other than SlyD are labeled for cells transformed with an empty vector control involving the pBAD/D-TOPO expression vector without introduction of the gene encoding RpoA*, indicating that the 42 kDa labeled protein is RpoA*. Consistent with this latter interpretation, a similar 42 kDa protein is labeled by **AsCy3_E** following purification of RpoA* (Figure S2 in Supporting Information). In all cases, specific labeling requires the biarsenical motif, as no labeling is apparent following cellular incubation with **2d** (**Cy3_E**), which does not contain an arsenical binding motif (Figure 2C). However, while **AsCy3_B** shows labeling specificity, robust and highly

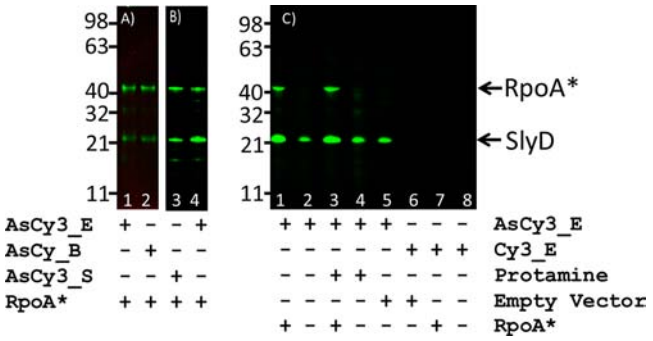

Figure 2. In vivo labeling of cytosolic bacterial proteins. Live cell labeling of *E. coli* in culture using 0.5 μM **AsCy3_E**, **AsCy3_B**, **AsCy3_S**, or **Cy3_E** for 30 min prior to cell lysis and separation of proteins using 4−12% Tris-Bis SDS-PAGE. (A,B) Selective labeling of SlyD (24 kDa) and RpoA* (42 kDa) using **AsCy3_E**, **AsCy3_B**, or **AsCy3_S** following induction of RpoA* expression. (C) Absence (lanes 2, 4, 5, 6, and 8) or presence (lanes 1, 3, and 7) of expressed RpoA* following live cell labeling in the absence (lanes 1−2, 5−8) or presence (lanes 3−4) of 50 μg/mL protamine commonly used to disrupt membranes.[31] Lanes 5−6 represent **AsCy3_E** or **Cy3_E** labeling of an empty vector control involving the pBAD/D-TOPO expression system without introduction of the gene encoding RpoA*. In all other cases, expression of tagged RpoA was induced by 1.0 mM arabinose (see Experimental Procedures). Images were collected using a FluorChem Q imager with Cy3 filters (λ_{ex} = 534 nm; λ_{em} = 606 nm).

reproducible labeling of RpoA* is problematic due to the formation of J-aggregates (Figure 1A).

To further assess cellular delivery of **AsCy3_E**, *E. coli* was incubated with subtoxic concentrations (50 μg/mL) of a 32 amino acid cationic peptide (i.e., protamine), previously shown to increase membrane permeability for small molecules (e.g., carboxyfluorescein) from loaded *E. coli* cells.[31] Under these conditions, there is minimal leakage of cytosolic proteins from *E. coli*, and cells remain viable.[31] Equivalent labeling of either SlyD or RpoA* by **AsCy3_E** is observed irrespective of membrane destabilization by protamine (Figure 2C), indicating that **AsCy3_E** readily partitions across the *E. coli* membranes to efficiently label cytosolic proteins. Depending on the relative abundance of expressed RpoA* relative to SlyD, there is substantial variation in the ability to detect labeled SlyD (see Figures S1 and S2 in Supporting Information). However, for experiments associated with cellular imaging we emphasized conditions that result in low abundances of RpoA*, where prior measurements have demonstrated the formation of foci containing supramolecular complexes involving RNA polymerase that form near the membrane under rapid growth conditions.[17,18,28,29]

A further comparison of the utility of **AsCy3_S** and **AsCy3_E** probes involved a side-by-side comparison of cellular labeling for *E. coli* expressing RpoA*. In the case of **AsCy3_S**, there is heterogeneous cellular labeling, resulting in a small fraction of the cellular population that is fluorescently labeled (Figure 3A). In comparison, **AsCy3_E** permits a more uniform cellular labeling in which the vast majority of cells are visible, enabling quantitative comparisons of protein labeling across a population of cells. In both cases, background labeling is low, as evidenced by the low nonspecific labeling for **2b** (**Cy3_S**) and **2d** (**Cy3_E**) (Figure 3B). In all cases, representative bright-field and fluorescent images were taken sequentially, where the focus was first set using the bright-field image prior to obtaining the fluorescence image. Variations in the brightness of the labeled

dx.doi.org/10.1021/bc300619m | *Bioconjugate Chem.* 2013, 24, 251−259

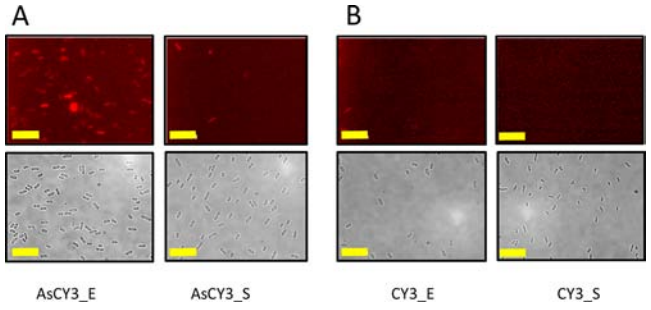

Figure 3. Targeted labeling for cellular imaging. Bright-field (bottom panels) and fluorescence (upper panels) images of *E. coli* expressing tagged RpoA* following incubation with 0.5 μM biarsenical cyanine probes **AsCy3_E** or **Cy3_E** (A) or controls (i.e., cyanine probes with no arsenics) (B). Yellow bar corresponds to ten micrometers.

cells arise due to (i) differences in the position of bacteria relative to the focal plane and (ii) heterogeneity in the abundance of the RNA polymerase complex (Figure S4). Differences in the sharpness of the images arise, in part, due to the fact that we are imaging living cells, where cells move during the collection of the fluorescent image (which takes about 1 s). In comparison, bright-field images were collected on the millisecond time-scale, during which there is minimal cell movement.

Resolution of RNA Polymerase Supramolecular Complexes. Visualization of site-specific labeling of the RNA polymerase is facilitated by the observation of supramolecular complexes that form near the membrane when cells are grown in rich media where ribosome biosynthesis is rate-limiting.[17,18,28,29] Under these conditions, a subpopulation of cells display bright foci located near the inner membrane (Figure 4A,B), as observed previously for the RNA polymerase complex in *E. coli* using a GFP fusion construct.[18] In comparison, only a diffuse staining is apparent for cells not expressing a tagged RpoA*, corresponding to the cellular distribution of cytosolic SlyD (Figure 4C). Observed foci are substantially brighter upon incubation of cells with **AsCy3_E** (Figure 4A) in comparison to **AsCy3_S** (Figure 4B), which is consistent with an enhanced cellular permeability. In the case of **AsCy3_E**, there is variation in the labeling intensity (Figure S4), which is consistent with previous observations that there is considerable heterogeneity in the abundance of expressed proteins within a cellular population;[32] alternatively, cells may exhibit differences in uptake. Arguing against this latter possibility are control experiments using **2b (Cy3_S)** and **2d (Cy3_E)** without an arsenical binding motif, which result in only a low diffuse background irrespective of the presence of tagged RpoA* (Figure 3B). Likewise, only diffuse staining is apparent when *E. coli* expressing tagged RpoA* is grown under conditions (i.e., minimal media) where supramolecular complexes of RNA polymerase do not form due to shifts in the distribution of actively transcribed operons.[28,29] These results demonstrate the utility of **AsCy3_E** for intracellular imaging experiments involving monitoring changes in supramolecular complex formation made possible by altering substituent moieties on the cyanine scaffold to reduce probe polarity and enhance intracellular delivery.

DISCUSSION

Optimal labeling of tagged cytosolic proteins is observed using the newly synthesized biarsenical probe **AsCy3_E**, which

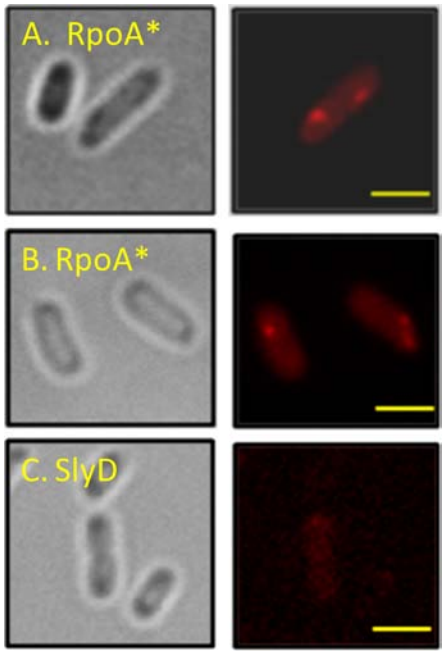

Figure 4. Resolution of supramolecular complexes of RNA polymerase. Bright-field (left panels) and fluorescence (right panels) following incubation of *E. coli* with 0.5 μM **AsCy3_E** (panels A and C) or **AsCy3_S** (panel B) in the presence of expressed RpoA* (A,B) or without induction when SlyD is selectively labeled (panel C). Yellow scale bar is 2 μm.

contains an ethanedithiol capping reagent with uncharged methoxy ester functionalized N-alkyl chains (Figures 2 and 3). Upon selective labeling of RpoA* with **AsCy3_E**, RNA polymerase is visualized to form a limited number of foci (Figure 4A), which is consistent with the formation of supramolecular protein complexes previously visualized using GFP-constructs.[18] A similar staining is observed using **AsCy3_S** (Figure 4B), albeit with reduced intensity that is consistent with reductions in cellular permeability (Figure 3). In comparison, a diffuse cellular staining is observed in the absence of expressed RpoA* that is associated with the selective labeling of the naturally occurring tetracysteine binding motif in SlyD, which is broadly distributed in the cytoplasm due to its general function as a peptidyl-prolyl cis−trans isomerase involved in the maturation of a large number of different proteins[33] (Figure 4C). The ability to resolve well-recognized molecular structures involving RNA polymerase complexes establishes the general utility of **AsCy3_E** for in vivo targeting and imaging of tagged intracellular bacterial proteins (Figure 4).

Biarsenical chemical probes remain the only current approach involving organic dyes that are in routine use for imaging intracellular proteins, requiring the simple introduction of a small tagging sequence for targeted site-specific labeling of intracellular proteins for imaging.[34] A major advantage of these chemical probes, in comparison to fluorescent proteins, is that they are substantially smaller, brighter, and more photostable.[34] Since the demonstration that chemical probes can be used to target intracellular proteins for live-cell imaging by Tsien's group in 1998,[10] the modular nature of the scaffold has permitted the installation of additional functionalities, including affinity capture, cross-linking, and enzyme activity switching through the ability to site-specifically modify the introduced 9−15 amino acid tagging sequence.[11,35] The ability to couple the

scaffold to deliver other functionalities, e.g., quantum dots,[36] or other chromophores permitting, for example, super-resolution imaging are possible using the ability of the biarsenical probe to selectively label introduced protein tags,[25,37,38] akin to other peptide tags that permit labeling using activity based approaches involving modification of enzyme substrates with a range of fluorophores.[39] Biophysical measurements of protein structure are facilitated by the tetracoordinate linkage between the introduced fluorophore and tagging sequence, permitting measurements of protein dynamics.[40−44] Likewise, engineering bipartite tagging sequences within interacting proteins permit in vivo imaging of their associations in response to environmental signals.[45,46] However, AsCy3 remains the only reported biarsenical dye with a brightness appropriate for single molecule measurements of cytosolic proteins.[40] In this respect, the development of a biarsenical cyanine dye with improved cell permeability (i.e., **AsCy3_E**) apparent even in bacterial cells, which typically require harsher procedures to enable the biarsenical dyes to cross the membrane in comparison to mammalian cells,[11] opens up a range of super-resolution imaging possibilities. For example, nonspecific labeling of surface lysines with a Cy3-Cy5 conjugate functionalized with a *N*-hydroxysuccinimide (NHS) ester have been developed that allow super-resolution imaging of surface structures.[37] Selective incorporation of Cy3-Cy5 conjugates into existing targeting schemes involving SNAP-tag surface-expressed labeled proteins has been demonstrated, but the large size of the modified Cy3-Cy5 substrate limited intracellular penetration.[47] Thus, in addition to selective targeting to a small peptide label, the smaller overall size of **AsCy3_E** represents a primary advantage for intracellular labeling, as conjugation with Cy5 does not substantially increase overall size and should facilitate intracellular partitioning of photoswitchable dyes for super-resolution imaging.[25]

In addition to the enhanced brightness, photostability, and small size of **AsCy3_E** relative to other common tagging approaches involving, for example, the use of autofluorescent proteins, a major advantage involves the ability to use relatively low concentrations (i.e., 0.5 μM) for targeted cellular labeling that arises as a result of the ability of biarsenical probes to bind with nanomolar or better affinities.[7,9] In comparison, enzyme-based conjugation methods typically require 20-fold higher substrate concentrations for probe delivery.[48,49] The requirement for lower levels of incubated probe for site-specific labeling lowers background fluorescence and increases imaging contrast. Additional contrast is possible due to substantial increases in fluorescence quantum yields upon binding biarsenical probes to target sequences,[7−9] which increases 3.5-fold for **AsCy3_E** (Table 1). Modifying the structure of the capping reagent has the potential to further decrease background fluorescence, as shown for **AsCy3_B** where the rigid structure of the 1,2-benzenedithiol cap reduces the quantum yield (Table 1). Upon binding, the capping reagent will be displaced, resulting in an enhanced fluorescence signal to provide high imaging contrast. Unbound probe, despite possible delivery concerns relating to nonspecific binding and/or partitioning into selected organelles, should retain the capping reagent to minimize background signals. Thus, in addition to introducing functionalities within the cyanine scaffold, the modularity of the arsenic capping reagent offers the flexibility to tailor the structure of the AsCy3 as a potential means to enhance imaging contrast.

The ability of target **AsCy3_E** to label cytosolic proteins has important practical applications, since all other biarsenical probes are built around similar scaffolds with interarsenic distances between 4.65 Å and 4.75 Å that target the same tagging sequences (i.e., CCPGCC).[7,10,11,14] In comparison, the substantially larger interarsenic distance of 14.5 Å within the cyanine scaffold enables the labeling of an orthogonal tagging sequence (i.e., CCKAEAACC) (Scheme 2), permitting multicolor measurements involving the simultaneous use of both classes of biarsenical probes for live cell measurements of protein−protein interactions. In this latter respect, the absorbance of **AsCy3_E** has substantial overlap with the fluorescence emission of commercially available FlAsH, thereby functioning as a suitable acceptor for fluorescence resonance energy transfer measurements.[9] An additional advantage of the cyanine dyes is derived from their well-understood photostability and insensitivity to environmental perturbations (e.g., pH) that enhance quantitative imaging applications.

In summary, the ability to selectively label tagged cytosolic bacterial proteins for live cell visualization using **AsCy3_E** provides a general method to monitor protein localization and dynamics. Further, like other biarsenical probes, the sole requirement for their use involves the introduction of a small tagging sequence; rapid site-specific labeling permits measurements of protein dynamics under conditions not routinely possible using fluorescent proteins (e.g., anaerobic conditions, trafficking into the periplasm).[50] Enhanced cellular delivery requires a net reduction in overall polarity of the Cy3 scaffold through the introduction of methoxyester linkages; following cellular delivery, endogenous esterases are expected to cleave the methoxyester moieties to form carboxylates whose increased solubility are expected to limit nonspecific protein associations and partitioning into membranes.

■ ASSOCIATED CONTENT

Supporting Information

Additional data are available comparing labeling specificities of **AsCy3_E** and **AsCy3_S** (Figure S1), demonstrating the specific labeling of RpoA* (Figure S2), measurements of the labeling stoichiometries (Figure S3), and showing variations in the abundance of RpoA* in foci within cellular populations (Figure S4). This material is available free of charge via the Internet at http://pubs.acs.org.

■ AUTHOR INFORMATION

Corresponding Author

*Tel: (509) 371-6949. E-mail: thomas.squier@pnl.gov. FAX: (509) 372-4732.

Notes

The authors declare no competing financial interest.

■ ACKNOWLEDGMENTS

This work was supported by an SBR FSFA by the Department of Energy (DOE) Office of Biological and Environmental Research (OBER) Genome Science Program. PNNL is a multiprogram National Laboratory operated by Battelle for the DOE under contract no. DE-AC05-76RLO 1830. The authors declare no competing financial interest.

REFERENCES

(1) George, N., Pick, H., Vogel, H., Johnsson, N., and Johnsson, K. (2004) Specific labeling of cell surface proteins with chemically diverse compounds. *J. Am. Chem. Soc. 126*, 8896−8897.

(2) Johnsson, N., and Johnsson, K. (2003) A fusion of disciplines: Chemical approaches to exploit fusion proteins for functional genomics. *ChemBioChem 4*, 803−810.

(3) Juillerat, A., Gronemeyer, T., Keppler, A., Gendreizig, S., Pick, H., Vogel, H., and Johnsson, K. (2003) Directed evolution of O-6-alkylguanine-DNA alkyltransferase for efficient labeling of fusion proteins with small molecules in vivo. *Chem. Biol. 10*, 313−317.

(4) Keppler, A., Pick, H., Arrivoli, C., Vogel, H., and Johnsson, K. (2004) Labeling of fusion proteins with synthetic fluorophores in live cells. *Proc. Natl. Acad. Sci. U.S.A. 101*, 9955−9959.

(5) Kindermann, M., Sielaff, I., and Johnsson, K. (2004) Synthesis and characterization of bifunctional probes for the specific labeling of fusion proteins. *Bioorg. Med. Chem. Lett. 14*, 2725−2728.

(6) Los, G. V., Encell, L. P., McDougall, M. G., Hartzell, D. D., Karassina, N., Zimprich, C., Wood, M. G., Learish, R., Ohana, R. F., Urh, M., Simpson, D., Mendez, J., Zimmerman, K., Otto, P., Vidugiris, G., Zhu, J., Darzins, A., Klaubert, D. H., Bulleit, R. F., and Wood, K. V. (2008) HaloTag: a novel protein labeling technology for cell imaging and protein analysis. *ACS Chem. Biol. 3*, 373−382.

(7) Adams, S. R., Campbell, R. E., Gross, L. A., Martin, B. R., Walkup, G. K., Yao, Y., Llopis, J., and Tsien, R. Y. (2002) New biarsenical ligands and tetracysteine motifs for protein labeling in vitro and in vivo: synthesis and biological applications. *J. Am. Chem. Soc. 124*, 6063−6076.

(8) Cao, H., Chen, B., Squier, T. C., and Mayer, M. U. (2006) CrAsH: a biarsenical multi-use affinity probe with low non-specific fluorescence. *Chem. Commun.(Camb)*, 2601−2603.

(9) Cao, H., Xiong, Y., Wang, T., Chen, B., Squier, T. C., and Mayer, M. U. (2007) A red cy3-based biarsenical fluorescent probe targeted to a complementary binding peptide. *J. Am. Chem. Soc. 129*, 8672−8673.

(10) Griffin, B. A., Adams, S. R., and Tsien, R. Y. (1998) Specific covalent labeling of recombinant protein molecules inside live cells. *Science 281*, 269−272.

(11) Pomorski, A., and Krezel, A. (2011) Exploration of biarsenical chemistry–challenges in protein research. *ChemBioChem 12*, 1152−1167.

(12) Kindermann, M., George, N., Johnsson, N., and Johnsson, K. (2003) Covalent and selective immobilization of fusion proteins. *J. Am. Chem. Soc. 125*, 7810−7811.

(13) Andresen, M., Schmitz-Salue, R., and Jakobs, S. (2004) Short tetracysteine tags to beta-tubulin demonstrate the significance of small labels for live cell imaging. *Mol. Biol. Cell 15*, 5616−5622.

(14) Griffin, B. A., Adams, S. R., Jones, J., and Tsien, R. Y. (2000) Fluorescent labeling of recombinant proteins in living cells with FlAsH. *Methods Enzymol. 327*, 565−578.

(15) Chen, B., Cao, H., Yan, P., Mayer, M. U., and Squier, T. C. (2007) Identification of an orthogonal peptide binding motif for biarsenical multiuse affinity probes. *Bioconjugate Chem. 18*, 1259−1265.

(16) Zurn, A., Klenk, C., Zabel, U., Reiner, S., Lohse, M. J., and Hoffmann, C. (2010) Site-specific, orthogonal labeling of proteins in intact cells with two small biarsenical fluorophores. *Bioconjugate Chem. 21*, 853−859.

(17) Verma, S., Xiong, Y., Mayer, M. U., and Squier, T. C. (2007) Remodeling of the bacterial RNA polymerase supramolecular complex in response to environmental conditions. *Biochemistry 46*, 3023−3035.

(18) Jin, D. J., and Cabrera, J. E. (2006) Coupling the distribution of RNA polymerase to global gene regulation and the dynamic structure of the bacterial nucleoid in *Escherichia coli*. *J. Struct. Biol. 156*, 284−291.

(19) Mujumdar, R. B., Ernst, L. A., Mujumdar, S. R., Lewis, C. J., and Waggoner, A. S. (1993) Cyanine dye labeling reagents: sulfoindocyanine succinimidyl esters. *Bioconjugate Chem. 4*, 105−111.

(20) Kanaya, S., Koyanagi, T., and Kanaya, E. (1998) An esterase from *Escherichia coli* with a sequence similarity to hormone-sensitive lipase. *Biochem. J. 332*, 75−80.

(21) Pacaud, M. (1982) Identification and localization of two membrane-bound esterases from *Escherichia coli*. *J. Bacteriol. 149*, 6−14.

(22) Jung, M. E., and Kim, W. J. (2006) Practical syntheses of dyes for difference gel electrophoresis. *Bioorg. Med. Chem. 14*, 92−97.

(23) Narayanan, N., and Patonay, G. (1995) A new method for the synthesis of heptamethine cyanine eyes - synthesis of new near-infrared fluorescent labels. *J. Org. Chem. 60*, 2391−2395.

(24) Olah, G. A., Hashimoto, I., and Lin, H. C. (1977) Electrophilic mercuration and thallation of benzene and substituted benzenes in trifluoroacetic acid solution. *Proc. Natl. Acad. Sci. U.S.A. 74*, 4121−4125.

(25) Fu, N., Xiong, Y., and Squier, T. C. (2012) Synthesis of a targeted biarsenical Cy3-Cy5 affinity probe for super-resolution fluorescence imaging. *J. Am. Chem. Soc. 134*, 18530−18533.

(26) West, W., and Pearce, S. (1965) The dimeric state of cyanine dyes. *J. Phys. Chem. 69*, 1894−1903.

(27) Mujumdar, R. B., Ernst, L. A., Mujumdar, S. R., Lewis, C. J., and Waggoner, A. S. (1993) Cyanine dye labeling reagents - sulfoindocyanine succinimidyl esters. *Bioconjugate Chem. 4*, 105−111.

(28) Cabrera, J. E., and Jin, D. J. (2003) The distribution of RNA polymerase in *Escherichia coli* is dynamic and sensitive to environmental cues. *Mol. Microbiol. 50*, 1493−1505.

(29) Cabrera, J. E., and Jin, D. J. (2006) Active transcription of rRNA operons is a driving force for the distribution of RNA polymerase in bacteria: effect of extrachromosomal copies of rrnB on the in vivo localization of RNA polymerase. *J. Bacteriol. 188*, 4007−4014.

(30) Wang, T., Yan, P., Squier, T. C., and Mayer, M. U. (2007) Prospecting the proteome: identification of naturally occurring binding motifs for biarsenical probes. *ChemBioChem 8*, 1937−1940.

(31) Johansen, C., Verheul, A., Gram, L., Gill, T., and Abee, T. (1997) Protamine-induced permeabilization of cell envelopes of gram-positive and gram-negative bacteria. *Appl. Environ. Microbiol. 63*, 1155−1159.

(32) Bar-Even, A., Paulsson, J., Maheshri, N., Carmi, M., O'Shea, E., Pilpel, Y., and Barkai, N. (2006) Noise in protein expression scales with natural protein abundance. *Nat. Genet. 38*, 636−643.

(33) Schmid, F. X., Mayr, L. M., Mucke, M., and Schonbrunner, E. R. (1993) Prolyl isomerases: role in protein folding. *Adv. Protein Chem. 44*, 25−66.

(34) Fernandez-Suarez, M., and Ting, A. Y. (2008) Fluorescent probes for super-resolution imaging in living cells. *Nat. Rev. Mol. Cell Biol. 9*, 929−943.

(35) Schepartz, A., and Gonzalez, R. L., Jr. (2011) Molecular imaging: sine labore nihil. *Curr. Opin. Chem. Biol. 15*, 749−751.

(36) Genin, E., Carion, O., Mahler, B., Dubertret, B., Arhel, N., Charneau, P., Doris, E., and Mioskowski, C. (2008) CrAsH-quantum dot nanohybrids for smart targeting of proteins. *J. Am. Chem. Soc. 130*, 8596−8597.

(37) Conley, N. R., Biteen, J. S., and Moerner, W. E. (2008) Cy3-Cy5 covalent heterodimers for single-molecule photoswitching. *J. Phys. Chem. B 112*, 11878−11880.

(38) Bhunia, A. K., and Miller, S. C. (2007) Labeling tetracysteine-tagged proteins with a SplAsH of color: a modular approach to bis-arsenical fluorophores. *ChemBioChem 8*, 1642−1645.

(39) Lukinavicius, G., and Johnsson, K. (2011) Switchable fluorophores for protein labeling in living cells. *Curr. Opin. Chem. Biol. 15*, 768−774.

(40) Scheck, R. A., and Schepartz, A. (2011) Surveying protein structure and function using bis-arsenical small molecules. *Acc. Chem. Res. 44*, 654−665.

(41) Chen, B., Mayer, M. U., Markillie, L. M., Stenoien, D. L., and Squier, T. C. (2005) Dynamic motion of helix A in the amino-terminal domain of calmodulin is stabilized upon calcium activation. *Biochemistry 44*, 905−914.

(42) Chen, B., Mayer, M. U., and Squier, T. C. (2005) Structural uncoupling between opposing domains of oxidized calmodulin underlies the enhanced binding affinity and inhibition of the plasma membrane Ca-ATPase. *Biochemistry 44*, 4737−4747.
(43) Chen, B., Mahaney, J. E., Mayer, M. U., Bigelow, D. J., and Squier, T. C. (2008) Concerted but noncooperative activation of nucleotide and actuator domains of the Ca-ATPase upon calcium binding. *Biochemistry 47*, 12448−12456.
(44) Roberti, M. J., Jovin, T. M., and Jares-Erijman, E. (2011) Confocal fluorescence anisotropy and FRAP imaging of alpha-synuclein amyloid aggregates in living cells. *PLoS One 6*, e23338.
(45) Halo, T. L., Appelbaum, J., Hobert, E. M., Balkin, D. M., and Schepartz, A. (2009) Selective recognition of protein tetraserine motifs with a cell-permeable, pro-fluorescent bis-boronic acid. *J. Am. Chem. Soc. 131*, 438−439.
(46) Luedtke, N. W., Dexter, R. J., Fried, D. B., and Schepartz, A. (2007) Surveying polypeptide and protein domain conformation and association with FlAsH and ReAsH. *Nat. Chem. Biol. 3*, 779−784.
(47) Maurel, D., Banala, S., Laroche, T., and Johnsson, K. (2010) Photoactivatable and photoconvertible fluorescent probes for protein labeling. *ACS Chem. Biol. 5*, 507−516.
(48) Gautier, A., Juillerat, A., Heinis, C., Correa, I. R., Jr., Kindermann, M., Beaufils, F., and Johnsson, K. (2008) An engineered protein tag for multiprotein labeling in living cells. *Chem. Biol. 15*, 128−136.
(49) Keppler, A., Gendreizig, S., Gronemeyer, T., Pick, H., Vogel, H., and Johnsson, K. (2003) A general method for the covalent labeling of fusion proteins with small molecules *in vivo*. *Nat. Biotechnol. 21*, 86−89.
(50) Xiong, Y., Chen, B., Shi, L., Fredrickson, J. K., Bigelow, D. J., and Squier, T. C. (2011) Targeted protein degradation of outer membrane decaheme cytochrome MtrC metal reductase in Shewanella oneidensis MR-1 measured using biarsenical probe CrAsH-EDT(2). *Biochemistry 50*, 9738−9751.